Skriver, E., Maunsbach, A. B., & Jørgensen, P. L. (1981) *FEBS Lett. 131*, 219–222.
Stryer, L. (1965) *J. Mol. Biol. 13*, 482–495.
Stryer, L. (1978) *Annu. Rev. Biochem. 47*, 819–846.
Taniguichi, K., Suzuki, K., & Iida, S. (1983) *J. Biol. Chem. 258*, 6927–6931.
Van Etten, R. L., Waymack, P. P., & Rehkop, D. M. (1974) *J. Am. Chem. Soc. 96*, 6782–6785.
Walderhaug, M. O., Post, R. L., Saccomani, G., Leonard, R. T., & Briskin, L. P. (1985) *J. Biol. Chem. 260*, 3852–3859.
Wallick, E. T., Lindenmayer, G. E., Lane, L. K., Allen, J. C., Pitts, B. J. R., & Schwartz, A. (1977) *Fed. Proc., Fed. Am. Soc. Exp. Biol. 36*, 2214–2218.
Wallick, G. T., Lane, L. K., & Schwartz, A. (1979) *J. Biol. Chem. 254*, 8107–8109.
Yguerabide, J. (1972) *Methods Enzymol. 26*, 498–578.
Yoda, A., & Yoda, S. (1982) *Mol. Pharmacol. 22*, 693–699.
Yoda, A., & Yoda, S. (1986) *J. Biol. Chem. 261*, 1147–1152.
Zampighi, G., Kyte, J., & Freytag, W. (1984) *J. Cell Biol. 98*, 1851–1864.

Binding and Hydrolysis of ATP by Cardiac Myosin Subfragment 1: Effect of Solution Parameters on Transient Kinetics†

Jo H. Hazzard and Michael A. Cusanovich*
Department of Biochemistry, University of Arizona, Tucson, Arizona 85721
Received April 21, 1986; Revised Manuscript Received September 3, 1986

ABSTRACT: Transient kinetic data of ATP binding and cleavage by cardiac myosin subfragment 1 (S1) were obtained by fluorescence stopped flow and analyzed by using computer modeling based on a consecutive, reversible two-step mechanism:

$$M_0 + ATP \underset{k_{21}}{\overset{K'_0 k_{12}}{\rightleftharpoons}} M_1{\cdot}ATP \underset{k_{32}}{\overset{k_{23}}{\rightleftharpoons}} M_{12}{\cdot}ADP{\cdot}P_i$$

where M_1 and M_{12} denote myosin species with enhanced fluorescence and $K'_0 = K_0/(K_0[ATP] + 1)$. The kinetic constants K_0, k_{12}, k_{23}, and k_{32} and the fractional contributions of M_1 and M_{12} to the total fluorescence are analyzed over a range of systematically varied solution parameters. The initial ATP binding equilibrium (K_0), which decreases with increasing pH, is facilitated by a positively charged protein residue with a pK of 7.1. An active-site charge of +1.5 is determined from the ionic strength dependence. The rate constants k_{12}, k_{23}, and k_{32} also exhibit pK's near neutrality but increase with increasing pH. The majority of the large (−54 kJ/mol) negative free energy of ATP binding occurs upon S1 isomerization, k_{12}, and a large increase in entropy (183 J/kmol at 15 °C) is associated with the cleavage step. The equilibrium constant for the cleavage step, K_2, is determined as 3.5 at pH 7.0, 15 °C, and 200 mM ionic strength. There are no significant changes in fractional contributions to total fluorescence enhancement due to solvent-dependent conformational changes of S1 in these data. When values for the combined rate constants are calculated and compared with those determined by graphical analysis, it is observed that graphical analysis overestimates the binding rate constant (K_0k_{12}) by 25% and the hydrolysis rate constant ($k_{23} + k_{32}$) by as much as 30%. Comparison of these data for cardiac S1 with available data for skeletal S1 indicates that the proteins have similar combined rate constants except for K_0k_{12}, which is approximately 7 times larger for skeletal S1. As the two proteins' electrostatic dependencies are similar, a steric constraint to nucleotide binding in the cardiac S1 relative to the skeletal S1 is postulated.

The mechanism of ATP binding and hydrolysis by myosin and its catalytic subfragment 1 (S1)[1] consists of at least three steps: (a) formation of a collision complex in rapid equilibrium with reactants followed by (b) an essentially irreversible conformational change resulting in an enhancement of fluorescence and (c) the rate-limiting step in which the γ-phosphate bond is cleaved, resulting in an additional fluorescence enhancement (Bagshaw & Trentham, 1974; Johnson & Taylor, 1978). This is given by the expression:

$$M_0 + T \underset{}{\overset{K_0}{\rightleftharpoons}} M_0{\cdot}T \underset{k_{21}}{\overset{k_{12}}{\rightleftharpoons}} M_1{\cdot}T \underset{k_{32}}{\overset{k_{23}}{\rightleftharpoons}} M_{12}{\cdot}D{\cdot}P_i \quad (1)$$

where M_0 is myosin S1, M_1 and M_{12} denote S1 with enhanced fluorescence, and T, D, and P_i refer to ATP, ADP, and inorganic phosphate, respectively. The product release steps can be considered separately from binding and hydrolysis as the first step in eq 2 is the overall rate-limiting step (Bagshaw &

$$M_{12}{\cdot}D{\cdot}P_i \underset{k_{43}}{\overset{k_{34}}{\rightleftharpoons}} M_{12}{\cdot}D + P_i \overset{K_4}{\rightleftharpoons} M_1{\cdot}D \overset{K_5}{\rightleftharpoons} M_0{\cdot}D \overset{K_6}{\rightleftharpoons} M_0 + D \quad (2)$$

Trentham, 1974; Johnson & Taylor, 1978) and is quite slow

† This research was supported in part by U.S. Public Health Service Grant HL 28906 to M.A.C. and NIH Postdoctoral Fellowship HL 07107 and American Heart Association, Arizona Affiliate, Grant-in-Aid to J.H.H.

[1] Abbreviations: S1, myosin subfragment 1; BTP, 1,3-bis[[tris(hydroxymethyl)methyl]amino]propane; DTT, dithiothreitol; HMM, heavy meromyosin; MES, 2-(*N*-morpholino)ethanesulfonic acid; HPLC, high-performance liquid chromatography.

0006-2960/86/0425-8141$01.50/0

(0.02 s^{-1}) (Taylor & Weeds, 1976; Smith & Cusanovich, 1984).

The complete mechanism has been developed and formulated on the basis of work with myosin from a single muscle type, skeletal, for which many of the rate constants under a variety of experimental conditions have been measured [reviewed in Taylor (1979)]. Attempts to extend detailed kinetic studies to cardiac myosin have been complicated by the greater lability of the cardiac protein which can result in kinetic heterogeneity, clearly observable in pre-steady-state experiments (Taylor & Weeds, 1976; Flamig & Cusanovich, 1981, 1983). Recent improvements in cardiac myosin S1 preparation and handling have minimized the problems of S1 aggregation, greatly simplifying the study of transient kinetics (Smith & Cusanovich, 1984). The available kinetic data, both from transient and from steady-state experiments, on the hydrolysis of ATP by cardiac myosin indicate that the cardiac protein follows the same mechanism as does skeletal myosin. For the rate constants that have been determined to date, however, some significant differences have been detected, i.e., K_0k_{12}, k_{34}, and k_{45} have been reported to be 3–4-fold slower for cardiac than for skeletal S1 (Flamig & Cusanovich, 1983; Smith & Cusanovich, 1984). Qualitatively, these results are consistent with the slower rate of contraction of cardiac relative to skeletal muscle (Barany, 1967; Delcayre & Swynghedauw, 1975).

In this report, the transient kinetics of ATP hydrolysis by bovine cardiac myosin S1 are examined over a range of temperatures, pHs, and ionic strengths. The resulting data are analyzed by using a computer modeling procedure in which the ATP dependence of the observed rate constant, the fluorescence vs. time curve at each ATP concentration, and the amplitude of the fluorescence enhancement are fit simultaneously for each data set to the rate expression for a consecutive, reversible, two-step process preceded by a rapid equilibrium. This analysis allows quantitation of the individual equilibrium and rate constants and of the fractional contribution of $M_1{\cdot}T$ and $M_{12}{\cdot}D{\cdot}P_i$ to the total fluorescence over a range of systematically varied solution parameters. The individual kinetic constants are shown to be strongly dependent upon pH, ionic strength, and temperature.

Experimental Procedures

Bovine cardiac myosin S1 was prepared by chymotryptic digestion of myosin (Smith & Cusanovich, 1984): the resulting S1 was free of myosin, HMM, and actin as determined by polyacrylamide gel electrophoresis in sodium dodecyl sulfate (Taylor & Weeds, 1976). The actin-activated ATPase activity for each S1 preparation was measured in a pH stat at pH 7.0 and 25 °C (White, 1982; Smith & Cusanovich, 1984) using cardiac actin prepared as a by-product of the myosin preparation. The S1 protein was lyophilized in the presence of a 6-fold molar excess of sucrose and stored at −20 °C until used. Concentrations in milligrams per milliliter were determined as follows: myosin, A_{280} = 0.53; actin, A_{280} = 1.15; S1, A_{280} = 0.64 with a light-scattering correction of 1.5 A_{320}. Ammonium sulfate absolute grade from Research Plus Labs, ATP grade II, and chymotrypsin type 1-S from Sigma were used in the S1 preparation. All other chemicals used in protein preparation were reagent grade.

Prior to kinetic analysis, the sufficient protein was dissolved in 50 mM BTP, 100 mM KCl, 0.1 mM DTT, and 0.02% NaN_3 buffer and dialyzed overnight vs. the buffer at 4 °C to remove sucrose. The resulting concentrated stock protein solution was clarified by centrifugation on the following day and stored on ice. The buffer and 5 mM ATP solutions were prepared daily and equilibrated to the desired reaction temperature in a thermostated bath before the pH was adjusted. The stock protein solution was diluted to 8 μM in the buffer of choice immediately prior to the experiments. Buffers and salts were reagent grade: ATP used for stopped flow was vanadium-free Sigma grade from equine muscle.

During the course of the pH dependence studies, it was noted that at higher pH values the fluorescence transients that were single exponentials at the beginning of a series of experiments would become biphasic over several hours. The presence of a slow phase in the fluorescence transient with a rate constant of about 1 s^{-1} has been previously reported for cardiac S1 (Smith & Cusanovich, 1984). The loss of the monophasic transient occurred even when a concentrated solution of S1 was stored on ice at pH 7 and only diluted in the appropriate high-pH buffer immediately prior to the experiment. This suggested a time-dependent destabilization of the S1 which became evident when the protein was exposed to more extreme solution conditions. Dialyzing the S1 overnight to remove the sucrose used in lyophilization resulted in a concentrated solution that was 16–20 h old by the time experiments were begun. However, when the sucrose was removed from S1 by gel filtration (Bio-Gel P-30) an hour prior to the experiments, such biphasic transients were not observed. Stability was maintained despite storage of a relatively dilute S1 solution on ice at the extreme pH values for several hours during the course of the experiments. The slow phase was also observed for intact cardiac myosin when the protein was dialyzed overnight.

The transient kinetic apparatus and methods of data collection and analysis used in this work have been described (Flamig & Cusanovich, 1983). The xenon arc lamp previously used (Flamig & Cusanovich, 1981) was replaced by a mercury arc lamp which provided more intensity at the excitation wavelength used (295 nm). The photomultiplier dynode voltage was typically 300 V which gave a 0.70-V buffer background. For each nucleotide concentration, 4–8 replicates of 200 data points were averaged and stored for further analysis. The first 150 data points were collected over a time span of approximately four half-lives, and the final 50 data points were collected over 2–8 s until the maximum fluorescence enhancement was attained. All 200 data points were used in the nonlinear least-squares fit to determine whether a single or double exponential best fit the data. In almost all cases, the entire fluorescence enhancement was fit with a single-exponential equation, and the k_{obsd} was then determined from the fit to the first 150 data points (corresponding to four half-lives). Data that were best fit by a double exponential indicated protein degradation as discussed above, and these data were not used. The explicit solution of a two-step mechanism preceded by a rapid equilibrium (see Appendix) was fit to the stopped-flow data to obtain values for the kinetic constants.

The effect of ionic strength on the rate and equilibrium constants for the binding of ATP was analyzed by using the parallel plate model (Watkins, 1984). Although in its general form the parallel plate model requires ion–ion, ion–dipole, and dipole–dipole terms to describe electrostatic interactions, it frequently can be reduced to its simplest form (ion–ion interaction) (Watkins, 1984; Meyer et al., 1984; Tollin et al., 1984). This form is given by

$$\ln [k(I)] = \ln k_\infty - V_{ii}X(I) \qquad (3)$$

where the electrostatic interaction energy $V_{ii} = \alpha D_e^{-1} Z_1 Z_2 r_{12} \rho^{-2}$ with α a constant (128.47), D_e the effective dielectric constant at the interaction domain, Z_1 and Z_2 the charges on the in-

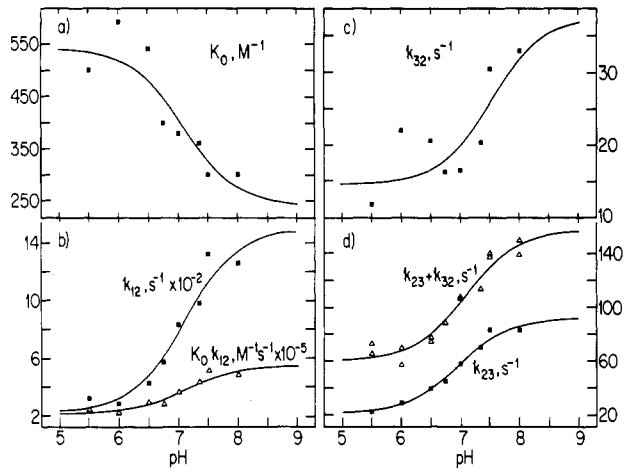

FIGURE 1: pH dependence of kinetic constants at 4 μM S1, 20 mM BTP, 20 mM MES, 10 mM $MgCl_2$, 0.1 mM DTT, 0.02% NaN_3, and KCl (concentration adjusted to give I = 200 mM) at 15 °C. Solid lines were drawn for the least-squares fits to the data assuming a single ionizing group and the following maximum and minimum kinetic constants: (a) 541 and 239 M^{-1} for K_0 (pK = 7.1); (b) 1.5 × 10^3 and 236 s^{-1} for k_{12} (pK = 7.1), 5.5 × 10^5 and 2.1 × 10^5 M^{-1} s^{-1} for K_0k_{12} (pK = 7.1); (c) 37.7 and 14.5 s^{-1} for k_{23} (pK = 7.5); (d) 156.9 and 59.6 s^{-1} for $k_{23} + k_{32}$ (pK = 7.1), 97.7 and 21.9 s^{-1} for k_{23} (pK = 7.1).

teraction domains of the reactions, r_{12} the distance between reactants (taken as the sum of van der Waals radii, 3.5 Å), ρ the radius of the interaction domain, $k(I)$ the observed second-order rate constant at ionic strength I, k_∞ the rate constant at infinite ionic strength, and $X(I)$ an ionic strength dependent term. The active-site charge was calculated by using an effective dielectric constant (D_e) of 20 as this is not unreasonable for a region where water is presumably excluded (Meyer et al., 1984).

The value of the equilibrium constant for the cleavage step, K_2, was determined by a rapid-quench technique (Bagshaw & Trentham, 1973). The reaction was initiated in a thermostated reaction vessel by adding 0.25 mL of 60 μM ATP in the standard BTP/MES/KCl buffer, pH 7.0, 15 °C, to 0.25 mL of 120 μM S1 in the same buffer. At 4 s, 0.50 mL of 7% perchloric acid at 4 °C was added to quench the reaction. The quench time was determined as the time required to attain maximum fluorescence in separate experiments with more dilute samples (S1 at 30 μM absorbed most of the 295-nm excitation light) in the stopped flow. The pH of the supernatant was adjusted to pH 6.0 ± 0.5 with NaOH. The sample was applied to a Pharmacia MONO-Q anion-exchange column attached to a Beckman Model 332 HPLC and eluted by using an ammonium phosphate buffer at pH 6.0 with a concentration gradient of 0.01–1 M over a 20-min period. The chromatography cleanly separated (3 min) ATP from ADP, which were detected at 257 nm with a Kratos Spectroflow 757 detector. The concentration ratio ADP/ATP was determined by peak integration using a Hewlett-Packard 3392A integrator. Control runs were those in which S1 was quenched prior to the addition of ATP.

RESULTS

Dependence of Kinetic Constants on Solution Parameters. The pH profiles for K_0, k_{12}, and k_{23} exhibit an n = 1 transition as expected for the ionization of a single group with a pK of 7.0–7.1 (Figure 1). The pK values for the substrate, $MgATP^{2-}$, are 1.49 and 4.00 (Alberty, 1968), far below neutrality. The ionizing group must therefore be considered to be a protein residue. K_0 decreases by 2-fold while k_{12} increases by 7-fold from pH 5.5 to 8.0. The decrease in K_0

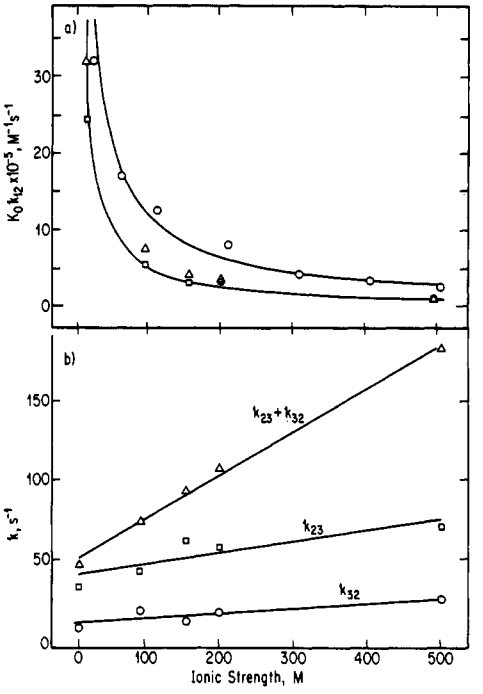

FIGURE 2: Ionic strength dependence of kinetic constants. Conditions for I = 10 mM were 2 μM S1, 5 mM BTP, 5 mM MES, and 4 mM $MgCl_2$; for I = 93 and 160 mM, 4 μM S1, 50 and 125 mM BTP, and 10 mM $MgCl_2$; for I = 200 and 500 mM, 4 μM S1, 20 mM BTP, 20 mM MES, 10 mM $MgCl_2$, and 138 and 500 mM KCl. All buffers contained 0.1 mM DTT and 0.02% NaN_3. Cardiac S1 values determined graphically (△) and by modeling (□) are shown. (a) K_0k_{12}, skeletal S1 data (○) from Johnson and Taylor (1978). The solid lines were calculated from the parallel plate equation (eq 3) with ρ = 3.5, D_e = 20, α = 128.47, and the charge on ATP = 2–. V_{ii} and the active-site charge were −5.15 kcal/mol and 1.4+, respectively, for skeletal S1, and −5.54 kcal/mol and 1.5+, respectively, for cardiac S1. (b) Rate constants for the hydrolysis step (which is unimolecular and therefore not analyzed by electrostatic theory); lines are linear least-squares fits.

with increasing pH is consistent with an electrostatic substrate-protein interaction which prefers a protonated species. In contrast, k_{23} and k_{32} are largest at high pH where the ionizable residue would be unprotonated. Although a distinct inflection point is not observed for k_{32} (Figure 1), its sensitivity to an increase in pH is 3-fold, similar to the 4-fold increase observed for k_{23}, and the pK is estimated as 7.5. The equilibrium constant K_2, as calculated from k_{23} and k_{32}, is relatively insensitive to pH, varying from 2 at low pH to a maximum of 3.5 at neutral pH and decreasing to 2.5 at high pH. Previous measurements for skeletal S1 have shown that K_2 is essentially pH independent over the range 7–8.5 (Bagshaw & Trentham, 1974), in agreement with the cardiac data reported here.

The ionic strength dependence of the graphical rate constants in Figure 2a is very similar to that observed for skeletal myosin S1 (Bagshaw et al., 1974; Johnson & Taylor, 1978). Analyses of both the cardiac binding rate constant and the corresponding skeletal data from Johnson and Taylor (1978) show the binding process to be of a plus/minus nature as described by electrostatic theory. The fit of the data to the parallel plate model given in eq 3 yields active-site charges of +1.5 and +1.4 for cardiac and skeletal S1, respectively (Figure 2). The modeling procedure shows the observed dependence of K_0k_{12} to be due entirely to a 23-fold decrease in K_0 in going from 10 to 500 mM ionic strength, k_{12} being independent of ionic strength.

As shown in Figure 2, $k_{23} + k_{32}$ increases linearly with increasing ionic strength when determined graphically.

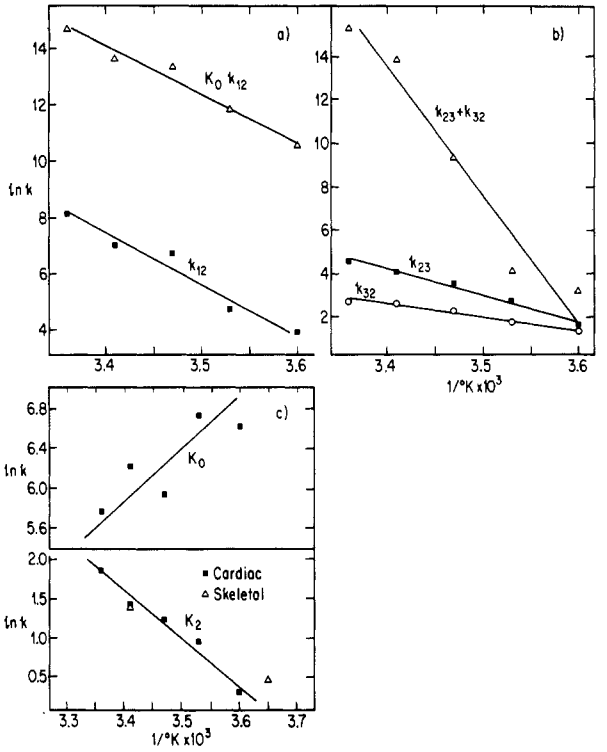

FIGURE 3: Temperature dependence of kinetic constants at 4 μM S1, 50 mM BTP, 10 mM $MgCl_2$, 0.1 mM DTT, and 100 mM KCl (I = 200 mM). The buffer pH was adjusted to 7.0 at each temperature. (a and b) Values determined graphically (△) and from modeling (■ and ○) are shown; (c) values for cardiac S1 determined from modeling (■); values for skeletal S1 (△) from Taylor (1977) and Johnson and Taylor (1978). The values at 20 and 3 °C were determined at pH 7.0 and 6.9, respectively. All lines are linear least-squares fits. Thermodynamic parameters calculated from these plots are given in Table I.

Table I: Thermodynamic Parameters

	Activation Parameters		
	ΔG^* (kJ mol^{-1}) at 15 °C	ΔH^* (kJ mol^{-1})	ΔS^* (J K^{-1} mol^{-1}) at 15 °C
cardiac k_{12}	55	146	317
cardiac k_{21}[a]	95		
cardiac k_{23}	61	98	131
cardiac k_{32}	64	57	−25
	Parameters from Equilibrium Constants		
	$\Delta G°$ (kJ mol^{-1}) at 15 °C	$\Delta H°$ (kJ mol^{-1})	$\Delta S°$ (J K^{-1} mol^{-1}) at 15 °C
cardiac K_0	−14	−30	−56
cardiac K_1[a]	−40		
skeletal K_0K_1[b]	−60	−100	−132
cardiac K_2	−3	50	183
skeletal K_2[b]	−5	80	297

[a] Estimated values (see text). [b] Values for $\Delta G°$, $\Delta H°$, and $\Delta S°$ from Kodama and Woledge (1979): conditions were pH 7.8, 23 °C, and 0.1 M KCl.

However, the dependence of $k_{23} + k_{32}$ derived from the modeling procedure is not as great: k_{23} increases 2-fold while k_{32} increases 3-fold. The resulting values for K_2 show no clear dependence on ionic strength (data not shown).

Thermodynamic parameters calculated from the Arrhenius plots of Figure 3 are given in Table I. Values for ΔH^* were calculated from the slope of the Arrhenius plot, ΔS^* from $R \ln k + \Delta H^*/T - R \ln (k_b T/h)$ (Jencks, 1969; Bray & White, 1966), and ΔG^* from $\Delta H^* - T\Delta S^*$. Values for $\Delta H°$ are from the slope of the van't Hoff plot, $\Delta G°$ from $-RT \ln K$, and $\Delta S°$ from $(-\Delta H° - \Delta G°)/T$. Values for ΔG^* for the graphical rate

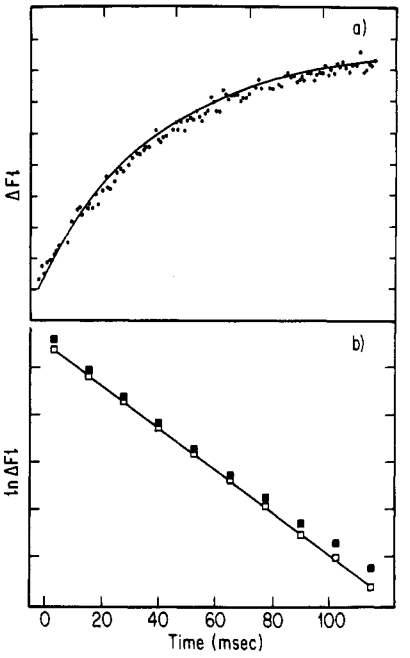

FIGURE 4: Comparison of calculated fluorescence vs. time with the stopped-flow trace for 2 mM ATP and 4 μM S1 at 5 °C. (a) ΔFl vs. time; solid line is calculated by using the parameters shown in Table AI. Data points are experimental. (b) ln ΔFl vs. time; calculated (■) and experimental (□) data are shown.

constants at 15 °C are 40 kJ mol^{-1} for binding (K_0k_{12}) and 60 kJ mol^{-1} for hydrolysis ($k_{23} + k_{32}$). Comparable values of 37 and 59 kJ mol^{-1}, respectively, were calculated from available skeletal S1 data (Chock et al., 1979). Thermodynamic parameters for the individual rate processes show that the initial binding of ATP to S1 is exothermic, with K_0 increasing with decreasing temperature, while the cleavage step is endothermic. That the binding process is exothermic and the cleavage process is endothermic has been demonstrated for skeletal S1 directly in calorimetric studies by Kodama and Woledge (1979). The results of their measurements for $\Delta H°$, $\Delta S°$, and $\Delta G°$ are given for comparison in Table I. An estimated value for K_1 can be made for cardiac S1 based on the value for k_{12} reported here and a value of 1×10^{-4} s^{-1} for k_{21} (Cardon & Boyer, 1978), which gives a value for K_1 of 1×10^7 at 20 °C, comparable to K_1 for skeletal myosin (10^7–10^8) (Taylor, 1979). This yields a $\Delta G°$ for the binding process (K_0K_1) of −54 kJ mol^{-1} which compares with −60 kJ mol^{-1} measured for skeletal S1.

It is anticipated that the transient fluorescence enhancement, being composed of two distinct steps, would develop a biphasic character under certain conditions in which the rate of binding (K_0k_{12}[ATP]) becomes significantly different from the rate of cleavage ($k_{23} + k_{32}$). Biphasic fluorescent transients have been reported for skeletal S1 at 5 °C (Johnson & Taylor, 1978). Distinctly biphasic transients are not observed with cardiac S1, even at solution extremes. This is not surprising, considering that the rate constants for binding and cleavage never differ by more than 2-fold in this study. The fluorescence vs. time curves generated by the computer modeling routine, however, do show some biphasic character. This is most clearly observed as a deviation from linearity in plots of ln Fl vs. time. Because this deviation falls within the noise level of the experimental trace, it is not observed, and the transient appears monophasic. An example of calculated data superimposed on experimental data at 5 °C is shown in Figure 4.

The value for the cleavage step equilibrium constant, K_2, as determined for skeletal S1 by quench experiments has been

Table II: Fluorescence Enhancement

	% ΔFl_0, $A_3 \times 100$	% $M_1 \cdot T$, $(A_2/A_3)/100$	% $M_{12} \cdot D \cdot P_i$, $[(A_3 - A_2) \times 100]/A_3$
*pH 7, 15 °C, 200 mM	27	37	63
pH variation			
5.5	21	71	29
*6.0	28	50	50
*6.5	28	39	61
*6.75	27	44	56
*7.35	27	37	63
7.5	25	32	68
8.0	21	29	71
temp (°C) variation (pH 7.0, I = 200 mM)			
5	22	73	27
10	20	65	35
*20	26	46	54
25	20	50	50
I (mM) variation (pH 7.0, 15 °C)			
10	23	13	69
*90	27	37	63
500	25	56	44
*av values[a]	27	41	59

[a] Values determined under normal solution conditions, denoted by asterisks, are averaged.

reported as 9 at pH 8.0 and 22 °C (Bagshaw & Trentham, 1973), as 1.6 at pH 6.9 and 3 °C (Taylor, 1977), and as 4 at pH 7 and 20 °C (Johnson & Taylor, 1978). The absolute numbers for the skeletal and cardiac (K_2 = 4.4, see below) equilibrium constants at neutrality and 20 °C compare well, and the temperature dependence for the two S1 types also is quite similar (Figure 3c). A value for K_2 for cardiac S1 has been reported as 11 at pH 8 and 25 °C (Taylor & Weeds, 1976). This value is substantially greater than that calculated here at pH 7 and 25 °C (6.4), and we find that K_2 is essentially independent of pH, so the values should be in agreement. The constant was therefore determined experimentally by a rapid-quench technique (see Experimental Procedures). The value for K_2 at pH 7.0 and 15 °C is measured as 4.4 which compares well with the calculated value of 3.5. The reason for the apparent discrepancy between the K_2 value reported here and that reported by Taylor and Weeds (1976) is not clear, but their value appears to be high. The reverse rate constant for cleavage, k_{32}, has been measured as 15 s^{-1} for skeletal S1 at pH 8.0, ionic strength 0.015 M and 20 °C, by oxygen-exchange experiments (Webb & Trentham, 1981). A direct comparison with values reported here is not possible, as solvent conditions differ and k_{32} is sensitive to pH and ionic strength as well as temperature. Cardiac values for k_{32} are 16.5 s^{-1} at pH 7.0, 0.2 M ionic strength and 15 °C, but increase to 33 s^{-1} at pH 8.0 and to 23 s^{-1} at 20 °C.

The temperature, ionic strength, and pH dependence of K_0 and k_{12} for skeletal S1 have been measured directly by a rapid-flow quench technique (Barman et al., 1983; Biosca et al., 1983). The results show a decrease in K_0 with decreasing temperature and ionic strength and a decrease in k_{12} with decreasing pH and ionic strength, in disagreement with the results reported here. The presence of 40% ethylene glycol in the quench flow experiments may contribute to this discrepancy.

Fluorescence Enhancement. Values for the total fluorescence enhancement, ΔFl_0, and the contribution of $M_1 \cdot T$ and $M_{12} \cdot D \cdot P_i$ to the total enhancement are given in Table II. The maximum ΔFl_0 is 27–29% and is observed at neutral pH from 15 to 20 °C at intermediate ionic strengths. There is no evidence in these data for significant changes in fluorescence enhancement due to solvent-dependent conformational changes of S1. Rather, the observed contribution of $M_1 \cdot T$ is dependent upon the magnitude of $K_0 k_{12}$, being lower at the higher values of the rate constants.

Discussion

Analyses of pre-steady-state kinetic data for the myosin S1–ATP system are almost exclusively based on graphical procedures which yield values for combined rate constants for ATP binding and cleavage. An alternative means of analysis of transient kinetic data employing computer modeling has been applied to this system in this report, and the computer-based kinetic constants have been compared with the graphics-based constants. Although the absolute values of the combined rate constants determined by graphical means are shown to be overestimates (Appendix), there is qualitatively no difference between graphical or computer-based values in terms of trends in combined kinetic constants with changes in solvent parameters. The computer modeling method, however, permits evaluation of individual kinetic constants rather than combined rate constants and also results in estimates for the relative contributions of the two fluorescence enhancement steps to the total fluorescence enhancement. Individual kinetic constants which have been determined directly by a variety of spectroscopic and chemical measurements are in good agreement with the computer modeling results reported here.

The protein active-site charge calculated from the ionic strength dependence of K_0 indicates that at least one protonated species is involved in the formation of the S1–ATP collision complex in both skeletal and cardiac S1. This type of ionic strength dependence has also been demonstrated for ADP binding to skeletal S1 (Trybus & Taylor, 1981) and would appear to be a general property of S1 nucleotide binding. The pH dependence of K_0, which shows a decrease in K_0 with increasing pH, is consistent with the ionic strength dependence if a basic residue (which would have a positive charge at low pH) is postulated at the active site. Thus, as the residue becomes unprotonated and uncharged, the binding equilibrium shifts to the right, favoring unbound reactants. This initial binding process proceeds with a decrease in entropy, as may be expected. The reaction is, however, exothermic, resulting in a negative free energy of reaction.

The ATP-induced conformational change in S1 (k_{12}) is insensitive to ionic strength but shows a strong dependence on pH, indicating that the isomerization is facilitated by an unprotonated amino acid residue with a pK similar to that for the initial binding. Although values for $\Delta H°$ and $\Delta S°$ cannot be calculated from these data due to the inability to estimate variations in k_{21} accurately, $\Delta G°$ can be determined from an estimated value for K_1. When the estimated $\Delta G°$ for K_1 is combined with the measured $\Delta G°$ for K_0, a value of −54 kJ mol^{-1} is obtained, which compares well with the value measured directly for skeletal S1 (−60 kJ mol^{-1}) (Kodama & Woledge, 1979). The ability to separate K_0 and K_1 shows that the majority of the large negative free energy of ATP binding occurs in the irreversible isomerization step rather than in the rapidly reversible initial collision.

As is the case for skeletal S1 (Kodama & Woledge, 1979), the endothermic cleavage step (K_2) is driven by a relatively large increase in entropy. The majority of the enthalpy and entropy changes occur in the forward reaction (k_{23}) from $M_1 \cdot T$ to the transition state. Therefore, the energy and structure of the activated complex can be said to more closely resemble that of the product, $M_{12} \cdot D \cdot P_i$. The increase in $k_{23} + k_{32}$ with

increasing ionic strength has previously been observed for skeletal S1 (Johnson & Taylor, 1978). In our study, a similar ionic strength dependence of the individual rate constants shows that k_{23} and k_{32} are affected to the same extent by ionic strength. The increase in k_{23} and k_{32} with ionic strength may be a result of a destabilization of the transition state between $M_1 \cdot T$ and $M_{12} \cdot D \cdot P_i$. The net effect of this destabilization would be to create a more rapid exchange between the two species without causing significant changes in the position of the equilibrium (K_2) or the stability of the $M_1 \cdot T$ and $M_{12} \cdot D \cdot P_i$ structures themselves. This latter condition is required by the relative insensitivity of the total fluorescence enhancement to ionic strength, indicating that the same $M_1 \cdot T$ and $M_{12} \cdot D \cdot P_i$ structures exist at any ionic strength.

The pH dependence of the rate constants for the cleavage step indicates that, as for the isomerization process, both cleavage and ATP synthesis are facilitated by one or more unprotonated residue(s) on the S1. The pK's of the pH dependencies of K_0, k_{12}, k_{23}, and k_{32} suggest the presence of at least one histidine residue in the protein active site. The data could also be explained by the anomalous ionization of another residue. The ionic strength dependence imposes the constraint that, in the case of K_0, it must be a basic residue that is being ionized. That a histidine important to hydrolysis is present in skeletal myosin has been inferred from the effects on the steady-state rate constant, k_{34}, of pH (Pelletier & Ouellet, 1961; Marsh et al., 1977), cations such as Zn (Hotta & Kojima, 1964), and chemical modification (Stracher, 1965; Hegyi & Muhlrad, 1968). The pH profiles reported here are in qualitative agreement with the pH dependence of the combined rate constants reported for skeletal S1 (Sleep et al., 1981).

On the basis of the pH dependencies of k_{12}, k_{23}, and k_{32} and assuming that the residue(s) involved is (are) a basic amino acid, proton release may be expected upon isomerization and upon cleavage. The largest proton release would be observed at lower pHs, where the residue is largely protonated prior to reaction. Proton release accompanying the transient fluorescence enhancement has been measured for skeletal S1 (Finlayson & Taylor, 1969; Chock & Eisenberg, 1974; Bagshaw & Trentham, 1974; Korentz & Taylor, 1975; Marsh et al., 1977; Chock, 1981), and the extent of proton release does decrease with increasing pH (Marsh et al., 1977). However, whether proton release occurs upon isomerization or cleavage has been a point of controversy. Our pH data indicate that proton uptake occurs upon ATP binding and that proton release occurs upon both isomerization and cleavage. This concomitant absorption and release of protons could complicate the proton release measurements. If proton release occurs only upon isomerization and not upon cleavage, it is reasonable to predict that K_2 will be independent of pH (Bagshaw & Trentham, 1974) and this appears to be the case for both skeletal (Bagshaw & Trentham, 1974) and cardiac S1. The analysis reported here which yields pH dependencies for k_{23} and k_{32} shows that the cleavage process (as well as the reverse process, synthesis) is pH dependent and that K_2 is pH independent only because of the very similar pH dependencies of the forward and reverse rate constants. Thus, proton release can be expected from the cleavage step even though K_2 is not pH dependent.

The entropy changes for both skeletal and cardiac S1 are substantial enough to suggest the presence of significant conformational changes during the processes of ATP binding and cleavage. Although there is a large (approaching 30%) total fluorescence enhancement occurring in going from $M_1 \cdot T$ to $M_{12} \cdot D \cdot P_i$, only local conformational changes that can be detected by UV absorption (Morita, 1967) and fluorometry (Werber et al., 1972) may be occurring. Spectroscopic data would suggest that the change in S1 structure upon nucleotide binding and hydrolysis is a localized event, involving perhaps only a few residues in the active site. No net alterations in helicity which would indicate a delocalized conformational change upon the formation of the steady-state complex of myosin, HMM, or S1 with ATP have been detected by circular dichroism or ORD spectroscopy (Kay et al., 1964; Gratzer & Lowey, 1969; Murphy, 1974; Cassim & Lin, 1975; McCubbin & Kay, 1982). The proton NMR spectrum of S1 is unaffected by ATP and ATP analogues (Highsmith et al., 1979). The entropy increases may also be explained by a decrease in the extent of ordered water structure surrounding the protein, as previously suggested by Kodama and Woledge (1979) as a result of the active-site tryptophan residues becoming more buried in the interior regions of the protein. However, chemical cross-linking studies have provided evidence that nucleotide binding can be communicated across distances as great as 28 Å (Wells & Yount, 1979; Perkins et al., 1981). Cross-linking of the two most reactive sulfhydryls in the presence of nucleotide results in a noncovalent trapping of the nucleotide even though the sulfhydryls are distant from the active site.

The picture of ATP binding and hydrolysis by cardiac S1 that emerges is of a rapid binding process in which loose electrostatic binding precedes tight binding with a large drop in free energy, followed by a slower cleavage step which is driven by an increase in entropy. Each step involves at least one protein residue which titrates close to neutrality. The characteristics of these pre-steady-state reactions and their intermediates appear to be very similar to available data for skeletal S1 with the exception of (a) the value for K_0, which is almost 7 times larger for the skeletal protein, and (b) the total fluorescence enhancement, which is one-third larger for skeletal S1. Values for k_{12}, k_{23}, k_{32}, and consequently K_2 are essentially the same for the two proteins. The most striking difference between cardiac and skeletal S1 is in the value for K_0, which must result from a difference in steric access to the nucleotide binding site as the overall ionic strength dependence, and thus the relevant electrostatics for nucleotide binding, is the same for both proteins.

Appendix

The minimum mechanism that describes the binding and hydrolysis of ATP by myosin S1 is a consecutive three-step process shown in eq 1. Although studies with ATP analogues and ADP indicate that the binding of ATP occurs in three rather than two steps (Garland & Cheung, 1979; Trybus & Taylor, 1982; Rosenfeld & Taylor, 1984; Smith & White, 1985), the presence of an additional step has no discernible effect on the analysis with ATP itself, and the minimum mechanism of eq 1 continues to provide the most straightforward means of analysis. It has been established that $k_{12} >> k_{23}$ (Johnson & Taylor, 1978) and that k_{21} is small [1×10^{-4} s^{-1} as measured by Cardon and Boyer (1978)]. It is generally agreed that $M_0 \cdot T$ is a collision complex in which the bound ATP is in rapid equilibrium with free ATP. Thus, eq 1 can be reduced to a two-step mechanism (Bagshaw & Trentham, 1974; Johnson & Taylor, 1978; Trybus & Taylor, 1982; Rosenfeld & Taylor, 1984):

$$M_0 + T \underset{k_{21}}{\overset{K'_0 k_{12}}{\rightleftharpoons}} M_1 \cdot T \underset{k_{32}}{\overset{k_{23}}{\rightleftharpoons}} M_{12} \cdot D \cdot P_i \qquad \text{(A1)}$$

where $K'_0 = K_0/(K_0[ATP] + 1)$. For the two-step mechanism, the fluorescence enhancement for the formation of $M_1 \cdot T$ is

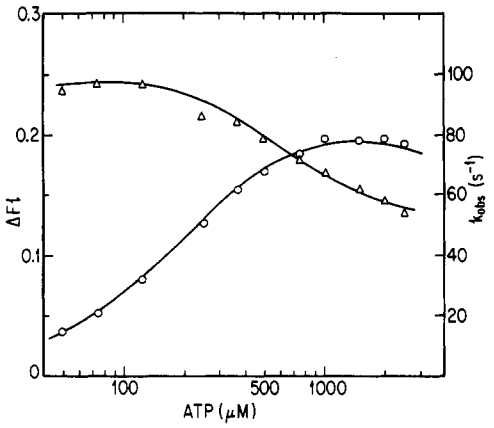

FIGURE A1: Fits for data obtained under standard solution conditions of pH 7.0, 15 °C, and 200 mM ionic strength. Plotted are the maximum fluorescence amplitude changes (ΔFl, t = 3 ms) (Δ) and observed pseudo-first-order rate constants (k_{obsd}) (O) vs. [ATP]. Solid lines are fits using parameters in Table AI.

given by eq A2, and the formation of M_{12}·D·P_i is given by eq A3:

$$\Delta Fl(M_1\cdot T) = (\lambda - \bar{k}_3)^{-1}(1 + K_2)^{-1}[(\bar{k}_3 - \lambda) \times (1 + K_2)\exp(-\lambda t) + \lambda K_2 \exp(-\bar{k}_3 t)] \quad (A2)$$

$$\Delta Fl(M_{12}\cdot D\cdot P_i) = K_2(K_2 + 1)^{-1}(\lambda - \bar{k}_3)^{-1}[\bar{k}_3 \exp(-\lambda t) - \lambda \exp(-\bar{k}_3 t)] \quad (A3)$$

where $\lambda = K'_0 k_{12}$, $\bar{k}_3 = k_{23} + k_{32}$, and t = time.

The fractional enhancement resulting from the formation of M_1·T is A_2, whereas A_3 is the sum of the enhancement due to the formation of M_{12}·D·P_i and M_1·T. The additional enhancement due to the formation of M_{12}·D·P_i is therefore $A_3 - A_2$. The total fluorescence change at any time t is then given by

$$\Delta Fl_t = A_2\Delta Fl(M_1\cdot T) + A_3\Delta Fl(M_{12}\cdot D\cdot P_i) \quad (A4)$$

For computer analysis, the values of the observed rate constant (k_{obsd}) and the corrected fluorescence enhancement (ΔFl_{corr}) at each [ATP] studied were used. ΔFl_{corr} is calculated by dividing the total observed voltage change on mixing S1 and ATP [multiplied by $\exp(k_{obsd}t_d)$, where t_d is 3 ms, the stopped-flow dead time] by the voltage at time zero (the voltage from S1 and buffer minus the voltage in the presence of buffer only). Thus, ΔFl_{corr} is the fluorescence enhancement extrapolated to t = 0, assuming that no other kinetic processes occur in the instrument dead time. Since all the reactions discussed here can be accurately described by a single exponential (within experimental error), we do not input the actual ΔFl_{obsd} vs. time data. Rather, this is calculated from k_{obsd} and ΔFl_{corr}.

Although there are seven unknowns (K_0, k_{12}[ATP], k_{21}, k_{23}, k_{32}, A_2, and A_3) for any particular data set, fitting the available data (k_{obsd} vs. [ATP] and ΔFl_{corr} vs. [ATP]) simultaneously greatly constrains possible values of the variables. The system is additionally constrained by the fact that the increase in ΔFl vs. time follows a single exponential at any [ATP] with SS1 and CS1. Since the mechanism requires two exponentials (assuming both have measurable fluorescence amplitudes), one process must occur in the stopped-flow dead time or the rates of the two processes must be similar (i.e., within a factor of 3). This fact reduces the number of possible fits. The very low value for k_{21} for myosin ATPase compared to values for the other rate constants further minimizes the number of error wells. In a typical fit, K_0, A_2, and A_3 are specified, and initial estimates of the four rate constants are made. The time course

Table AI: Representative Values of Kinetic Parameters Determined by Computer Modeling[a]

parameter	temp (°C) 5	15	20
K_0 (M^{-1})	750	380	500
k_{12} (s^{-1})	50.8	834	1.1×10^3
k_{23} (s^{-1})	8.5	57.3	97.0
k_{32} (s^{-1})	6.2	16.5	23.2

[a] The value of k_{21} is held at 1×10^{-4} s^{-1}. Solution conditions are pH 7.0, I = 200 mM.

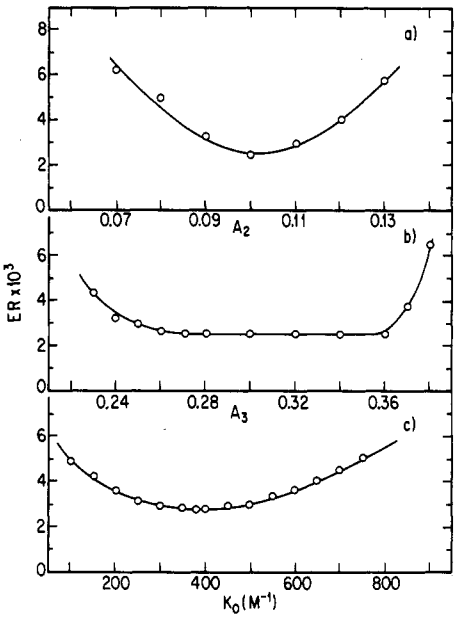

FIGURE A2: Error parameters for the fit in Figure A1. (a) A_3 and K_0 fixed at 0.27 and 380 M^{-1}, respectively. (b) A_2 and K_0 fixed at 0.10 and 380 M^{-1}, respectively. (c) A_2 and A_3 fixed at 0.27 and 0.10, respectively.

for the reaction is then calculated as well as the rate constant at each ATP concentration (k_{calcd}) and the total fluorescence change (ΔFl_{corr}). The calculated and observed data are then compared, and the least-squares error is minimized by varying the rate constants. Thus, for a particular value of K_0, A_2, and A_3, a best fit is obtained. This procedure is repeated for a series of K_0, A_2, and A_3 values, and the values of the individual parameters that yield the minimum least-squares error are reported. The fits for both k_{obsd} and fluorescence amplitude dependence on ATP concentration under standard conditions of pH 7, 15 °C, 200 mM ionic strength in BTP/MES buffer are illustrated in Figure A1. The modeling results reflect the nonhyperbolic behavior of k_{obsd} including the slight decrease in k_{obsd} at high [ATP] as well as the decrease in ΔFl_{corr} with increasing [ATP]. The average point to point error (obtained from the difference in calculated and observed values) is ±1% for k_{obsd} and ±2% for ΔFl_{corr}. The kinetic parameters resulting from this fit are listed in Table AI along with results from fits at 5 and 20 °C. The average point to point errors for ΔFl and k_{obsd} at 5 °C are 2.1% and 5.6%, respectively, and at 20 °C are 3.2% for ΔFl and 5.5% for k_{obsd}.

Well-defined error wells are produced for A_2 and K_0 by using this iterative procedure, as shown in Figure A2. A least-squares minimum is observed at 0.10 for A_2 and at 380 M^{-1} for K_0. In contrast, the error well for A_3 is broad and relatively undefined. As A_3 is increased above 0.26, k_{23} decreases and k_{32} increases; thus, K_2 decreases. This has no effect on the quality of the fits and reflects an intrinsic limitation of fitting a multiple parameter system. Measurement of K_2

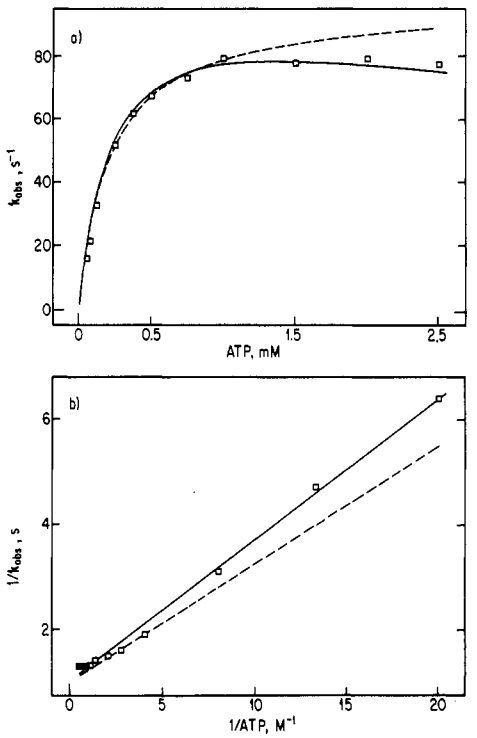

FIGURE A3: Dependence of k_{obsd} on [ATP] at pH 7.0, 15 °C, I = 200 mM. (a) The solid line is the computer-based fit; the dashed line is a hyperbolic fit to intermediate ATP concentrations. (b) Double-reciprocal plots for both curves in (a). The differences in slopes and y intercepts are 25% and 3%, respectively.

under these solution conditions using chemical quenching (Experimental Procedures) indicates that the best value for A_3 is 0.27 or the minimum value, found at the leading edge of the error well.

The standard deviation for the values of A_2 and A_3 and the kinetic constants has been estimated by varying the parameter in question while holding all others constant. The resulting error wells are well-defined and substantially deeper than those obtained with the iterative procedure (Figure A2), in which the values for the rate constants are permitted to float. The 90% confidence limits of each parameter are set as the variation in the parameter that results in a 50% increase in the total least-squares error (Johnson, 1983). At pH 7.0, 15 °C, and 200 mM ionic strength, the following standard deviations are estimated: 7% for K_0, 11% for A_2, 2% for A_3, 7% for k_{12}, 5% for k_{23}, and 12% for k_{32}.

Pre-steady-state kinetic data are more commonly analyzed in terms of combined rate constants for ATP binding (K_0k_{12}) and cleavage ($k_{23} + k_{32}$). These constants are calculated by using graphical procedures which assume a hyperbolic dependence of the observed rate constant, k_{obsd}, on ATP concentration [examples include Johnson & Taylor (1978), Chock et al. (1979), and Flamig & Cusanovich (1983)]. The graphical method can, at best, only estimate values for the rate constants as the dependence of k_{obsd} on ATP concentration is not, in fact, hyperbolic, as previously demonstrated for skeletal S1 by Johnson & Taylor (1978). The degree of departure from a hyperbolic dependence in the case of cardiac S1 is illustrated in the upper panel of Figure A3. The resulting double-reciprocal plot (lower panel) is therefore not linear and will not yield accurate values for K_0k_{12} and $k_{23} + k_{32}$.

As expected, the rate constants determined by the computer modeling technique differ in magnitude from those determined graphically: the value for K_0k_{12} from the model averages 75% of the value determined graphically, and the value for $k_{23} + k_{32}$ from the model averages 92% of the value determined graphically. The degree of overestimation of $k_{23} + k_{32}$ by the graphical method is dependent upon two factors: the magnitude of the binding rate constant and the percent M_1·T. When K_0k_{12} is small, i.e., less than 2×10^5 M^{-1} s^{-1}, and the percent M_1·T is high (50–75% of the total fluorescence change), the value for $k_{23} + k_{32}$ determined by modeling is only 70% of that determined graphically. The modeling $k_{23} + k_{32}$ is also lower than the maximum k_{obsd} under these conditions, which correspond to low temperature (5–10 °C), low pH (5.5–6.0), and high ionic strength (500 mM). When K_0k_{12} is large, i.e., greater than 1×10^6 M^{-1} s^{-1}, and the percent M_1·T is of intermediate or low value (30–50% of the total fluorescence change), the value for $k_{23} + k_{32}$ determined by modeling is 99% of that determined graphically. These latter conditions correspond to high temperature (25 °C) and low ionic strength (10 mM). Thus, graphical analysis cannot determine $k_{23} + k_{32}$ independently of K_0k_{12} under most conditions. The binding process is apparently contributing significantly to k_{obsd} at high [ATP], even when the value for k_{obsd} appears to have leveled off. The continued decrease in observed ΔFl as the [ATP] is increased beyond the level required for maximum k_{obsd} is consistent with this. The k_{obsd} would then equal $k_{23} + k_{32}$ only at very high [ATP], where its value would have decreased from the maximum k_{obsd}. This is indeed the case for skeletal myosin, where k_{obsd} decreases in value at very high [ATP] (Johnson & Taylor, 1978). This phenomenon is not observed to a significant extent for cardiac S1 under the conditions of these experiments as the cardiac binding rate constant is approximately 7-fold lower than that for skeletal S1.

Unlike $k_{23} + k_{32}$ the magnitude of the overestimation of the graphical K_0k_{12} does not depend upon values for fluorescence amplitude or rate constants or ratios of rate constants. The 25% average discrepancy between K_0k_{12} values determined by the two methods is therefore considered to be a matter of accuracy rather than a more complicated problem of separation of rate constants. The determination of K_0k_{12} from a double-reciprocal plot that is nonlinear, especially at higher [ATP], yields a slope that is too shallow and consequently a rate constant that is too large.

Registry No. ATP, 56-65-5; ATPase, 9000-83-3.

REFERENCES

Alberty, R. A. (1968) *J. Biol. Chem. 243*, 1337–1343.
Bagshaw, C. R., & Trentham, D. R. (1973) *Biochem. J. 133*, 323–328.
Bagshaw, C. R., & Trentham, D. R. (1974) *Biochem. J. 141*, 331–349.
Bagshaw, C. R., Eccleston, J. F., Eckstein, F., Goody, R. S., Gutfreund, H., & Trentham, D. R. (1974) *Biochem. J. 141*, 351–364.
Barany, M. (1967) *J. Gen. Physiol. 50*, 197–216.
Barman, T. E., Hillaire, D., & Travers, F. (1983) *Biochem. J. 209*, 617–626.
Biosca, J. A., Travers, F., & Barman, T. E. (1983) *FEBS Lett. 153*, 217–220.
Bray, H. G., & White, K. (1966) *Kinetics and Thermodynamics in Biochemistry*, J. and A. Churchill Ltd., London.
Cardon, J. W., & Boyer, P. D. (1978) *Eur. J. Biochem. 92*, 443–448.
Cassim, J. Y., & Lin, T.-I. (1975) *J. Supramol. Struct. 3*, 510–519.
Chock, S. P. (1981) *J. Biol. Chem. 256*, 10954–10960.
Chock, S. P., & Eisenberg, E. (1974) *Proc. Natl. Acad. Sci. U.S.A. 71*, 4915–4919.

Chock, S. P., Chock, P. B., & Eisenberg, E. (1979) *J. Biol. Chem. 254*, 3236–3243.
Delcayre, C., & Swynghedauw, B. (1975) *Pfluegers Arch. 355*, 39–47.
Finlayson, B., & Taylor, E. W. (1969) *Biochemistry 8*, 802–810.
Flamig, D. P., & Cusanovich, M. A. (1981) *Biochemistry 20*, 6760–6767.
Flamig, D. P., & Cusanovich, M. A. (1983) *J. Biol. Chem. 258*, 977–983.
Garland, F., & Cheung, H. C. (1979) *Biochemistry 18*, 5281–5289.
Gratzer, W. B., & Lowey, S. (1969) *J. Biol. Chem. 244*, 22–25.
Hegyi, G., & Muhlrad, A. (1968) *Acta Biochim. Biophys. Acad. Sci. Hung. 3*, 425–428.
Highsmith, S., Akasaka, K., Konrad, M., Goody, R., Holmes, K., Wade-Jardetzky, N., & Jardetzky, O. (1979) *Biochemistry 18*, 4238–4244.
Hotta, K., & Kojima, S. (1964) *J. Biochem. (Tokyo) 55*, 486–493.
Jencks, W. P. (1969) *Catalysis in Chemistry and Enzymology*, McGraw-Hill, New York.
Johnson, K. A. (1983) *J. Biol. Chem. 258*, 13825–13832.
Johnson, K. A., & Taylor, E. W. (1978) *Biochemistry 17*, 3432–3442.
Kay, C. M., Green, W. A., & Oikawa, K. (1964) *Arch. Biochem. Biophys. 108*, 89–98.
Kodama, T., & Woledge, R. C. (1979) *J. Biol. Chem. 254*, 6382–6386.
Koretz, J. F., & Taylor, E. W. (1975) *J. Biol. Chem. 250*, 6344–6350.
Marsh, D. J., de Bruin, S. H., & Gratzer, B. (1977) *Biochemistry 16*, 1738–1742.
McCubbin, W. D., & Kay, C. M. (1982) *Methods Enzymol. 85*, 676–698.
Meyer, T. E., Watkins, J. A., Przysiecki, C. T., Tollin, G., & Cusanovich, M. A. (1984) *Biochemistry 23*, 4761–4767.
Morita, F. (1967) *J. Biol. Chem. 242*, 4501–4506.
Murphy, A. J. (1974) *Arch. Biochem. Biophys. 163*, 290–296.
Pelletier, G. E., & Ouellet, L. (1961) *Can. J. Chem. 39*, 1444–1453.
Perkins, W. J., Wells, J. A., & Yount, R. G. (1981) *Biophys. J. 33*, 149a.
Rosenfeld, S. S., & Taylor, E. W. (1984a) *J. Biol. Chem. 259*, 11908–11919.
Rosenfeld, S. S., & Taylor, E. W. (1984b) *J. Biol. Chem. 259*, 11920–11929.
Sleep, J. A., Trybus, K. M., Johnson, K. A., & Taylor, E. W. (1981) *J. Muscle Res. Cell Motil. 2*, 373–399.
Smith, S. J., & Cusanovich, M. A. (1984) *J. Biol. Chem. 259*, 9365–9368.
Smith, S., & White, H. (1985) *J. Biol. Chem. 260*, 15146–15155.
Stracher, A. (1965) *J. Biol. Chem. 240*, PC958–PC960.
Taylor, E. W. (1977) *Biochemistry 16*, 732–740.
Taylor, E. W. (1979) *CRC Crit. Rev. Biochem. 6*, 103–164.
Taylor, R. S., & Weeds, A. G. (1976) *Biochem. J. 159*, 301–315.
Tollin, G., Cheddar, G., Watkins, J. A., Meyer, T. E., & Cusanovich, M. A. (1984) *Biochemistry 23*, 6345–6349.
Trybus, K. M., & Taylor, E. W. (1982) *Biochemistry 21*, 1284–1294.
Watkins, J. A. (1984) Ph.D. Thesis, University of Arizona.
Webb, M. R., & Trentham, D. R. (1981) *J. Biol. Chem. 256*, 10910–10916.
Wells, J. A., & Yount, R. G. (1979) *Proc. Natl. Acad. Sci. U.S.A. 76*, 4966–4970.
Werber, M. M., Szent-Gyorgyi, A. G., & Fasman, G. D. (1972) *Biochemistry 11*, 2872–2883.
White, H. D. (1982) *Methods Enzymol. 85*, 698–708.